THE US KEY PROJECT ON AGN SPECTRAL ENERGY DISTRIBUTIONS (CHARACTERISTICS OF THE ISO DATA)

E. Hooper[1], B. Wilkes[1], K.K. McLeod[2], M.S. Elvis[1], C. Impey[3], C. Lonsdale[4], M. Malkan[5], & J. McDowell[1]

[1] Harvard-Smithsonian Center for Astrophysics. Cambridge, MA, USA
[2] Wellesley College, Wellesley, MA, USA
[3] Steward Observatory, Tucson, AZ, USA
[4] IPAC, Caltech, Pasadena, CA. USA
[5] UCLA, Los Angeles, CA, USA

ABSTRACT

The US ISO Key Project on quasar spectral energy distributions seeks to better understand the very broad-band emission features of quasars from radio to X-rays. A key element of this project is observations of 72 quasars with the ISOPHOT instrument at 8 bands, from 5 to 200 μm. The sample was chosen to span a wide range of redshifts and quasar types. This paper presents an overview of the analysis and reduction techniques, as well as general trends within the data set (comparisons with IRAS fluxes, uncertainties as a function of background sky brightness, and an analysis of vignetting corrections in chopped observing mode). A more detailed look at a few objects in the sample is presented in Wilkes et al. (these proceedings).

Key words: ISOPHOT; infrared astronomy; quasars; spectral energy distributions.

1. INTRODUCTION

A substantial fraction of the bolometric luminosity of many quasars emerges in the infrared (Elvis et al. 1994), from synchrotron radiation and dust. Which of these emission mechanisms is dominant depends on quasar type and is an open question in many cases. Two major ISO observing programs have obtained broad-band photometry for large samples of quasars: a European Central program which focused on low-redshift, predominantly radio-loud quasars; and a US Key Project to examine quasars spanning a wide range of redshifts and SEDs, e.g., X-ray and IR-loud, plus those with unusual continuum shapes.

The final sample for the US Key Project consists of 72 quasars observed with the ISOPHOT instrument (Lemke et al. 1996) in most or all of the following bands: 5, 7, 12, 25, 60, 100, 135, and 200 μm. Ninety percent of the quasars in the sample have redshifts $z < 1$, while the remaining 10% lie in the range $2 < z < 4.7$ (see Hooper et al. 1999 for a plot of absolute blue magnitude vs. redshift for the sample). More than half of the sample consists of luminous X-ray sources, 25% are strong UV emitters, and smaller subgroups contain strong infrared sources, X-ray-quiet objects, red quasars, and BALQSOs. The infrared data points will be combined with all available fluxes at other wavebands to generate a comprehensive atlas of broadband SEDs (see Wilkes et al. in these proceedings for some examples).

Most of the sources (53 of 72) were observed in a rectangular chop mode, the point source detection technique preferred at the beginning of the ISO mission. Concerns about calibrating and interpreting chopped measurements, particularly at long wavelengths, led us to switch to small raster scans. We reobserved 18 of the chopped fields in raster mode and added 19 new targets. The change in observing strategy, combined with lower than expected instrumental sensitivity, has resulted in a halving of the originally planned sample. However, we now have the added benefits of data from both observing modes for a subset of the targets and better information about background variations from the raster maps.

In this paper we present an overview of the analysis and reduction strategies and give an update of the status of the data products. Reduction of faint object data taken with the ISOPHOT instrument has been complex and somewhat uncertain, and the techniques are still in a state of development. Comparisons of our results with independent checks, such as IRAS, and an overlap of the raster and chopped observing methods help establish the validity of our data set, and the large size of the sample provides a convenient testbed for a variety of analysis procedures.

2. POINT SOURCE FLUXES

The bulk of the data reduction, including most instrumental calibrations and corrections, is done with PIA, the standard software for ISOPHOT reductions

Proceedings of the Conference "The Universe as seen by ISO", Paris, France, 20–23 October 1998 (ESA SP-427, March 1999)

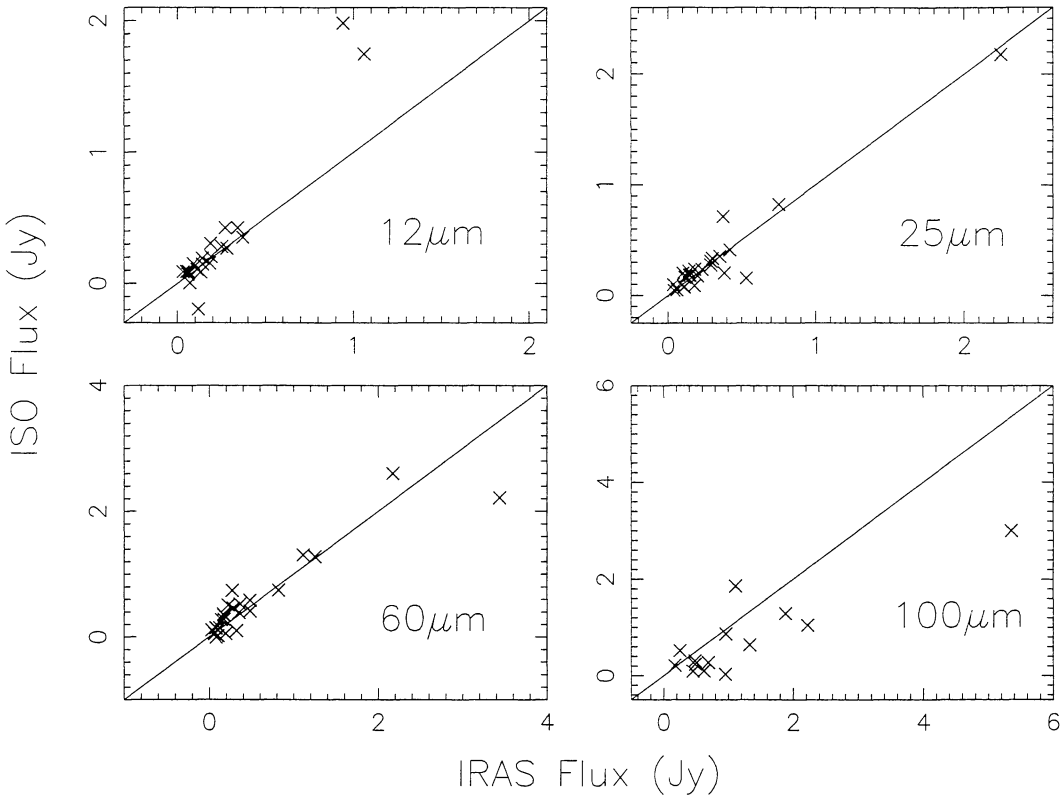

Figure 1. Comparison of ISO and IRAS fluxes for chopped measurements reduced with a Fourier transform code. Lines corresponding to equal flux observed with both telescopes are provided to guide the eye and do not represent any kind of fitting.

(Gabriel, Acosta-Pulido, & Heinrichsen 1998). Basic steps are typically run in batch mode, including ramp subdivision into 8 points per pseudo-ramp, two-threshold deglitching, orbitally dependent dark current subtraction, and flux calibration with the internal fine calibration sources, to produce AAP-level files. Standard instrumental drift corrections have not been employed in chopped data, as there are too few points per chopper plateau. We have not yet explored the use of drift corrections in raster data. The AAP files are left without vignetting corrections or sky subtraction, as these steps are done with external custom scripts.

The final reduction steps, extracting the source flux and estimating uncertainties, is an area of ongoing work, with multiple techniques being explored. To maintain flexibility, IDL scripts outside of PIA, written by Martin Haas & Sven Müller and modified by us, are used for both chopped and raster data. We currently employ three main techniques: a traditional source minus the average of adjacent backgrounds for chopped data, from which are derived numerous statistics; a Fourier analysis of the sequence of chopped measurements, which is generally less affected by residual glitches than the traditional approach but is more difficult to interpret; and a simple average background subtraction in the raster maps to obtain source flux and uncertainty estimates. Many on-the-fly options are available, including altering the vignetting values, finding and correcting gaps in the chopper sequence, discarding part of the sequence, flat fielding, background subtraction, plus plots of any aspect of the data.

Fluxes derived using the Fourier transform analysis of chopped measurements of relatively bright sources are compared to IRAS values in Figure 1. The agreement is generally good; possible explanations for the few large deviations include residual glitches or flux calibration errors in ISO, errors in IRAS fluxes, or intrinsic source variation. A similar plot was presented in Hooper et al. (1999) based on an earlier stage of the analysis techniques. An improvement in the agreement of the ISO and IRAS fluxes in the current version is particularly apparent at 60 μm.

3. BACKGROUND ESTIMATES

Intrinsic sky structure noise can dominate instrumental uncertainties in ISOPHOT measurements at wavelengths $\lambda \geq 100\mu$m (Herbstmeier et al. 1998). Background fluctuations are particularly problematic for simple chopped measurements with the four-pixel C200 array, where they contribute a systematic error that is difficult to determine directly from the observations. One possibility is to estimate the structure noise using the results of Herbstmeier et al. (1998), along with the prescription of Helou & Beichman

(1990) to adjust for the observed sky brightness and selected wavelength.

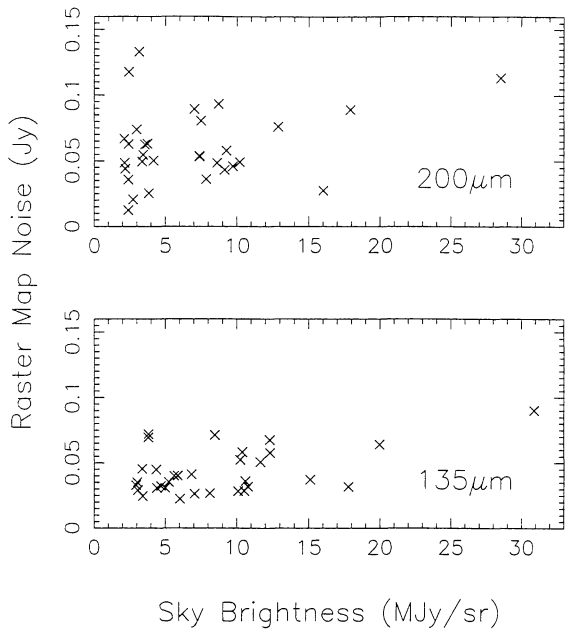

Figure 2. Rms noise vs. sky brightness for the C200 array raster data, calculated from off-source positions in the same manner as the flux for the source. Includes contributions from both the instrumental noise and the sky structure noise.

We measure the background variations more directly where possible from 2×4 raster scans with the C200 array, using the same technique as the source flux determination. The difference between the flux at a sky position in the raster sequence and the average of the preceding and following pointings (cases in which the source is centered on the pixel in any of these three positions are excluded) for each pixel forms a sequence of 12 measurements from which to estimate the total noise contribution, including structure noise and instrumental effects. These noise figures are plotted against measured sky brightness in Figure 2 for most of the raster maps in our sample. A weak trend of increasing noise with sky brightness is evident at 200 μm. The results are generally consistent with Herbstmeier et al. (1998), given that extrapolations of the structure noise between different fields and brightness levels can differ from the measured values by a factor of 5 or more.

4. VIGNETTING CORRECTIONS

Vignetting corrections are important parameters for chopped faint source observations, as relatively small errors can produce large changes in the computed source flux. Working with Martin Haas, we derived vignetting corrections from our C200 chopped data (135 & 200 μm) to compare with the default values.

The first step was to calculate average flat fields for the array in the on and off-source positions separately. Given the large sample size, we expect that any observed differences in the measured flat fields reflect changes in the vignetting between the two chopper positions. With proper vignetting corrections applied, the values should be close for each pixel. This was not the case for the default corrections; the flat fields differed by a similar or larger factor than with no correction applied at all.

The ratios of the on and off-source flat fields were used to estimate vignetting corrections, a process aided by the geometry of the array and the chopper motion. All of the observations had a rectangular chopping pattern of $\pm$90 arcsec, a total throw approximately equal to the projected angular size of the array. The spacecraft pointed halfway between the source and the background field. In this configuration, one half of the array imaged the central field of view of the spacecraft in each chopper position. Assuming that the central field had relatively uniform low-level vignetting (in the calculations it is set to 1.0, the same value used for the central field with no chopper movement), the flat field ratios directly gave the vignetting correction factors for the outer part of the chopping pattern. The derived corrections, listed in Table 1, are smaller and more uniform than the standard values, which range from 1.01 to 1.10. In addition, the new numbers are smaller at the longer wavelength, whereas many but not all of the default corrections follow the opposite trend. We are still evaluating whether the new or standard vignetting corrections are closer to the true values.

Table 1. Vignetting corrections for the C200 array with a total chopper throw of 180 arcsec. Derived from the average flat fields of each pixel in the on-source (+90 arcsec chopper position) and off-source (-90 arcsec chopper position) configurations.

λ & chop position	Pixel 1	Pixel 2	Pixel 3	Pixel 4
135 μm on source	1.018	1.000	1.000	1.024
135 μm off source	1.000	1.026	1.015	1.000
200 μm on source	1.009	1.000	1.000	1.010
200 μm off source	1.000	1.022	0.999	1.000

ACKNOWLEDGMENTS

Martin Haas, Sven Müller, Mari Poletta, and Ann Wehrle provided invaluable help with the data reduction. We benefited greatly from discussions with Thierry Courvoisier, Péter Ábrahám, Ilse van Bemmel, Rolf Chini, and Bill Reach. The IDC, IPAC, and the INTEGRAL Science Data Center were very hospitable during visits to work on this project. The financial support of NASA grant NAGW-3134 is gratefully acknowledged.

REFERENCES

Gabriel, C., Acosta-Pulido, J., & Heinrichsen, I. 1998 Proc. of the ADASS VII conference, ASP Conf. Ser. 145, ed. R. Albrecht, R.N. Hook, & H.A. Bushouse (San Francisco: ASP), 165

Helou, G., & Beichman, C. A. 1990, in "From Ground-Based to Space-Borne Sub-mm Astronomy," Proc. of the 29th Liége Internat. Astroph. Coll. (ESA), 117

Herbstmeier, U. et al. 1998, A&A, 332, 739

Hooper, E., Wilkes, B., McLeod, K., McDowell, J., Elvis, M., Malkan, M., Lonsdale, C., & Impey, C. 1999, in "Astrophysics with Infrared Surveys: A Prelude to SIRTF," ed. M. Bicay, R. Cutri, & B. Madore (San Francisco: ASP), in press

Lemke, D. et al. 1996, A&A, 315, L64